POLITECNICO DI TORINO
Repository ISTITUZIONALE

Ultrasonic measurements for assessing the elastic parameters of two-component grout used in full-face mechanized tunnelling

Original
Ultrasonic measurements for assessing the elastic parameters of two-component grout used in full-face mechanized tunnelling / Todaro, C., Godio, A., Martinelli, D., Peila, D.. - In: TUNNELLING AND UNDERGROUND SPACE TECHNOLOGY. - ISSN 0886-7798. - ELETTRONICO. - 106:103630(2020). [10.1016/j.tust.2020.103630]

Availability:
This version is available at: 11583/2852162 since: 2020-11-11T10:35:58Z

Publisher:
Elsevier

Published
DOI:10.1016/j.tust.2020.103630

Terms of use:

This article is made available under terms and conditions as specified in the corresponding bibliographic description in the repository

Publisher copyright

(Article begins on next page)

10 June 2026

Ultrasonic measurements for assessing the elastic parameters of two-component grout used in full-face mechanized tunnelling

Carmine Todaro, Alberto Godio, Daniele Martinelli, Daniele Peila

DIATI–Politecnico di Torino, Corso Duca degli Abruzzi 24, 10129 Torino, Italy

Abstract

The use of shield machines and instantaneous segment linings for tunnel construction is one of the most used tunnelling methods today. Despite a large number of applications in different tunnelling projects all around the world, knowledge of the behaviour of two-component grout is quite limited, mainly due to the fast hardening process that inhibits using the classic approach for concrete characterization. In the present work, an innovative approach based on ultrasonic measurements is introduced, aimed to characterize the elastic properties of this innovative backfilling material. Specifically, ultrasonic pulse velocity was applied to two-component grout samples to describe the interesting and fast evolution of the material from the mixing phase until 6 months of curing using geophysics parameters. The dynamic Young's modulus (E) and the dynamic shear modulus (G) exhibited a clear increasing trend, starting from values of a few tens of MPa to final values equal to 1000 MPa and 340 MPa, respectively. The Poisson's ratio (ν), close to the value of incompressible materials (0.5) at the short curing time, exhibited a decreasing trend, reaching roughly 0.445 after 3 months of curing.

Keywords: EPB, Two-component grout, Backfilling, Elastic Modulus, Grout mechanical parameters

1. Introduction

The use of shield TBMs, especially in urban areas, requires particular attention to avoid surface settlement. An important aspect to avoid this problem is effectively filling the annular gap, called backfilling, left between the lining and the surrounding soil (Figure 1). Furthermore, the backfilling must lock the assembled segments into the right position, avoiding movement due to both segment self-weight and thrust forces generated by the TBM advancement. A contribution to bear the loads transmitted by the TBM backup weight is given from the injected material that also ensures a uniform, homogeneous and immediate contact between the ground and the lining itself. Consequently, a symmetrical and homogeneous solicitation loading along the lining avoids puncture loads and the backfilling contribution to the waterproofing of the whole system is preserved (Pelizza et al., 2010; Peila et al., 2011, 2015; Ivantchev and Del Rio, 2015; ASTM, 2016; Shah et al., 2018). Different technologies and materials can be used for the backfilling operation, as discussed by Pellegrini and Perruzza (2009); Thewes and Budach (2009); Novin et al. (2015). The three main products are inert mix, cement mix and two-component mix, as reported in EFNARC (2005); Youn and Breitenbücher (2014).

[Figure 1 about here.]

Among other technologies, the two-component mix is widely used thanks to its technical and operative advantages. It is composed of a superfluid mortar, stabilized to guarantee its workability for a long time, usually at least 72 hours, to which an accelerator admixture is added at the injection point (Hashimoto et al., 2004; Pellegrini and Perruzza, 2009; Dal Negro et al., 2017). The mix starts to harden a few seconds after the addition of the accelerator (exhibiting a thixotropic consistency similar to a gel). The developing of a certain mechanical strength is almost instantaneous, weaker compared to standard concrete but sufficient to bear the machine backup, as described in ITATech (2014).

Despite many applications worldwide (Peila et al., 2015), knowledge of the mechanical behaviour of this technology is quite limited, mainly due to the quick hardening time. Very limited indications are available about two-component backfilling elastic properties, such as the elastic moduli and Poisson's ratio, especially considering their evolution as a function of curing. In Thewes and Budach (2009) it is merely stated that the backfilling material should exhibit a stiffness modulus similar to that of the excavated medium (5–10 MPa) but, unfortunately, no reference to the curing time or a procedure useful for laboratory assessment is provided. Càmara (2018), referring to the Follo Line project, reports the design requirement of Young's modulus higher than 20 MPa after 2 hours and higher than 100 MPa after 4 hours. This work has crucial importance since it highlights the scientific gap concerning the elastic behaviour of two-component grout. It introduces the current engineering demand of certain values of Young's modulus at short curing times (up to 1–2 hours, which represents a crucial stage of backfilling for the correct design and numerical modelling) and also underlines the absence of a reliable method for computing it. It should be stated that standard test procedures used in structural or geotechnical engineering cannot be applied to the two-component material for two main reasons. First, the

hardening reaction is so quick that the same test procedure cannot follow the evolution of the process (properties of the mixed grout change continuously and quickly until 3 hours after casting), and second, the obtained values are so small compared to the ones proper to ordinary cement that the error using standard equipment is not negligible.

In conclusion, at present, no information related to the elastic behaviour of two-component grout is available in the scientific literature, despite this information recently starting to be listed in the technical specifications of construction sites and as acceptance criterion (Càmara, 2018). Furthermore, no data related to real case histories are available; consequently, the order of magnitude of the elastic parameters, especially at short curing time, is also presently unknown. To overcome this scientific gap, non-destructive geophysical procedures were adopted to assess the elastic behaviour of these two-component mixtures immediately after casting and curing time (Green, 1991; Basu and Aydin, 2006). The research was developed to assess the P-wave and S-wave travel times on two-component grout specimens for different curing times. Values of the dynamic Young's modulus (E), dynamic shear modulus (G), Poisson's ratio (ν) and bulk modulus (K) were computed. The adjective "dynamic", according to the geophysical discipline, highlights that the obtained parameters were achieved with infinitesimal samples strains; the dynamic elastic parameters should not be confused with the "static" ones (Agrò et al., 2009). Outcomes at short curing time (few hours) and long curing time (3–6 months) are presented separately to highlight the different nature of two-component grout during different ageing phases.

2. General aspects of two-component mix technology

Two-component mix technology is based on mixing two fluids (hereinafter called component A and component B) that maintain their liquid status from the batching station (usually located on the job field yard) to the machine. The different pipelines run along the tunnel path, enter through the machine back up and reach specific tanks, expressly designed with volumes suitable for guaranteeing the needed material for at least one machine advance step (Zarrin et al., 2015). These fluids mix a few centimetres before the output nozzles, circularly installed on the shield tail (Pelizza et al., 2012; Dal Negro et al., 2017; Todaro et al., 2019, 2020).

Component A is made up of cement, bentonite and a retarding/fluidising agent even if some further components are also admitted. For example, the use of polymers suitably designed for replacing bentonite has spread in recent years. Moreover, as described in Schulte-Schrepping and Breitenbücher (2019), furnace slag, fly ash and metakaolin are also starting to be added to component A. The constituents are sourced from "industrial" production and so they should be perfectly controlled; this production automation guarantees regularity of the raw materials in terms of composition with obvious advantages in the engineering properties constancy of both fresh fluids and hardened mixes. Usually, standard cement Type I is used, except in the case of different design specifications. The most used bentonite in Europe is sodic and its use significantly increases the homogeneity and the waterproofing of the hardened mix. Furthermore, if correctly activated, it plays the main role in minimizing the bleeding of component A. Concerning the retarding agent, it has a plasticizing effect and it can inhibit the mortar from setting, thereby guaranteeing its workability for up to 72 hours after batching. This facilitates stockpiling the grout in the mixer containers, which are larger than the theoretical volume of material to be injected per ring (Dal Negro et al., 2017). This is useful for avoiding one of the most common job field critical issues, namely batching and stockpiling only the theoretical backfilling volume. In other words, if an unexpected larger void is eventually found, the two-component volumes available on the machine backup should ensure the complete backfilling operation, avoiding potentially serious consequences. Component B consists of an accelerator admixture usually made up of sodium silicate and water with different mutual percentages.

When the two components are mixed, the reaction start and just a few seconds are required to obtain a gel (Thewes and Budach, 2009; Pelizza et al., 2010). The time-lapse that occurs between mixing and the end of the gelling process is called the "gelling time" and it can be managed by changing the mutual volume proportion between components A and B, as depicted in Figure 2.

[Figure 2 about here.]

3. General aspects of two-component mix technology

In the following, a description of the work carried out is provided.

3.1. International standards

The European Standard on ultrasonic measurements for concrete defines the method for determining the propagation velocity of ultrasonic longitudinal waves in hardened concrete. The velocity can be used for determining concrete uniformity, the presence of cracks or voids, changes in properties with time and dynamic physical properties.

CEN (2004), particularly, gives guidance on testing fresh concrete, hardened concrete and concrete in structures, specifying a method for the velocity determination of ultrasonic longitudinal waves. Moreover, it provides additional information on the main factors affecting the pulse velocity measurements and the correlation between pulse velocity and strength. For this study, ASTM (2016) was also consulted. This standard defines determining the propagation velocity of longitudinal stress waves through concrete, overlapping the prescriptions of CEN (2004) that was the base regulation followed.

Despite both the abovementioned standards recommending to ensure a sufficient coupling pressure between sample surfaces and transducers, no base value is mentioned. However, some useful indications are provided in standards concerning determining the sound propagation speed in natural stone or rocks. Specifically, ISRM (1977) was taken into account and the minimum pressure value of 0.1 MPa was considered a minimum value for the sample-transducers coupling.

3.2. The testing method used: Ultrasonic pulse velocity (UPV)

The ultrasonic pulse velocity (UPV) method is widely used to detect internal defects, estimate the crack depth and assess the compressive strength of concrete elements (Strurrup et al., 1984). Standard test methods for UPV measurements are well established in the technical literature (McCann and Forde, 2001; Popovics, 2003). According to the standards, the UPV of the first arrival wave (longitudinal and shear waves) is determined through a specific wave path, and the dynamic mechanical properties of the material under test are estimated (Khan et al., 2011).

In concrete testing, transducers with a frequency range between 20 and 100 kHz and a 54 kHz centre frequency are typically used. The test is performed by attaching two transducers to the concrete surface and measuring the transmission time and velocity of longitudinal waves between them. The transducer arrangement for UPV inspections can be classified into three categories, direct transmission (cross probing), semi-direct transmission and indirect transmission (surface probing). These methods are based on the propagation of longitudinal vibration pulses, which are produced by an electro-acoustical transducer. Finally, the vibration pulses are converted into an electrical signal by a second transducer and the transit time can be measured.

At the laboratory scale, the commonly adopted method is direct transmission where the transmitter and the receiver transducers are usually located on the two opposite faces of a specimen (usually a cylinder-shaped specimen). In such a case, the frequency range between 100 kHz and 200 kHz can be adopted.

The accuracy in estimating the UPV depends on several factors (Aydin, 2014):

- accuracy in preparing the specimen and in the determination of its length;
- the quality of the coupling between the transducer and the specimen;
- the electronic noise of the received signal.

Taking into account the abovementioned factors about geophysics methods, the accuracy in the determination of the material density also strongly affects the quality of the final outcomes.

3.3. Sampling manufacturing

The geophysical test campaign was performed by using the following mix design (Table 1).

[Table 1 about here.]

To obtain a component A with properties close to the one manufactured in a batching station of the job site at the laboratory scale (Todaro et al., 2021), the procedure described in Todaro et al. (2019) was followed.

Once component A has been produced, the reciprocal volume percentage of both components (Table 1) were metered, mixed and the obtained mix was immediately poured in the mould (Figure 3). Cylindrical moulds (composed by two coupled halves of commercial PVC PN 16 with 52 mm internal diameter, 130 mm height, 5.4 mm thickness and density ranging between 1.35 and 1.46 kg/l) were used for samples tested at short curing time while prismatic ones were used for long term tests (according to CEN (2016)).

[Figure 3 about here.]

Cylindrical moulds were used due to the poor mechanical strength of young gelled two-component grout. By using this mould, only the two surfaces for transducers were without cover and the samples can be handled without damage during test arrangement and execution.

Both the moulds used for the campaign are depicted in Figure 3. The size of the cylindrical samples was chosen according to (CEN, 2004). This standard requires a minimum recommended length of 100 mm for testing concrete samples characterized by 20 mm nominal aggregates. The two-component technology does use aggregates; however, it is common to find air bubbles (max dimension of 5 mm for laboratory-scale samples) embedded inside the hardened grout. Therefore, assuming parallelism between standard concrete aggregates and air bubbles (in both cases wave propagation alteration occurs) a height of about 130 mm was chosen for cylindrical moulds. The 52 mm diameter respects the B5 annexe of CEN (2004) concerning the least lateral dimension of tested samples. The chosen geometry was also in accordance with CEN (2016).

Taking into account the procedure developed for preparing the samples used for short term analysis Todaro et al. (2019), after casting, a plastic film was put on the free surface to avoid dehydration during the scheduled curing time. For samples used for long term analyses, the plastic film covered the free surface for 24 hours, whereupon the curing process was started, putting the demoulded specimens in water with an average temperature of 23±2°C.

After every demoulding operation, the sample density values (ρ) were assessed and an average value of 1.206 kg/l with a variance (σ^2) of $4.157 \cdot 10^{-4}$ was observed. This value was used as the reference for all geophysical computations. After the density assessment, an optical check of each sample was carried out to discharge damaged specimens. The suitable ones started the curing process steeped in water.

3.4. Apparatus

All the geophysical tests were performed using a Pundit® PL-200, a fully integrated device expressly designed for ultrasonic pulse velocity tests coupled with a pair of transducers with a 250 kHz natural frequency. This device incorporates the pulse generator, receiver amplifier and a time measuring circuit. Other authors (Zarei et al., 2019) successfully adopted similar apparatus.

4. Test campaign

4.1. Testing procedures

Tests were performed using UPV with a direct transmission approach.

Cylindrical specimens were used for analysing short curing time. Samples were tested in a direct transmission arrangement without removing the PVC moulds (Figure 4). A pressure of about 0.4 MPa (according to ISRM (1977)) was applied through a laboratory press, taking care to avoid excessive transducer penetrations inside the two free surfaces of the sample. The procedure was optimized to ensure good mechanical coupling and minimize the loss of energy at the interface between the transducers and the specimen.

[Figure 4 about here.]

A preliminary calibration is required when measuring using shear wave transducers. This step was done using a small amount of specific coupling gel on the transducers and pressing them on either side of a calibration rod. Care was taken to distribute the coupling gel properly and homogeneously to avoid having air trapped between the transducer and the calibration rod.

During the measurements with the 250 kHz shear wave transducers, a special shear wave coupling paste was adopted. It is a non-toxic, water-soluble organic substance with a very high viscosity, allowing shear waves to be properly transmitted into the object under test.

It is important to highlight that measurements with shear wave transducers require perfect alignment of the two transducers. This constraint is because shear waves are generated in a single plane only. Rotating one of the transducers with respect to the second one is a good way to check the propagation of the shear wave; when the two transducers are out of phase of 90°, the shear wave signal is minimized or disappears. In general, misaligned transducers provide almost no S-wave component while correctly aligned transducers should produce a very strong S-wave component.

By simultaneously measuring the travel times of the longitudinal and shear waves generated at ultrasonic frequency (up to 250 kHz) at different time steps, the evolution of the two-component gelled grout was studied in terms of geophysical parameters.

For analysing samples cured a long time, prismatic samples were used and the above-mentioned procedure was followed as well, with the exception of the confinement pressure that was increased to 1 MPa.

4.2. Data processing

Basic processing was performed to estimate the first arrival of the longitudinal and shear wave travel times. The processing flow was based on displaying the signal as wiggle traces, application of automatic gain control to recover energy, band-pass filtering to remove unwanted electronic noise, and finally, manually picking the travel times was carried out.

By measuring the P-wave and S-wave travel times, the bulk modulus (K) and dynamic shear modulus (G) were determined using Equations 1 and 2, respectively:

$$K = \rho V_p^2 - \frac{4}{3}G \tag{1}$$

where ρ is the density of the material and V_p is the pulse velocity of the P-wave;

$$G = \rho V_s^2 \tag{2}$$

where Vs is the pulse velocity of the S-wave.

Poisson's ratio was determined using Equation 3, by measuring the P-wave velocity and the S-wave velocity. It is important to underline the independence of this parameter from the material density.

$$v = \frac{V_p^2 - 2V_s^2}{2V_p^2 - 2V_s^2} \tag{3}$$

Once Poisson's ratio is known, the dynamic Young's modulus can be calculated using Equation 4:

$$E = 2G(1 + n) \tag{4}$$

4.3. Results

As discussed in Hashimoto et al. (2004) and Antunes (2012), despite the hardened process of the two-component grout continuing over the time from the mixing phase, two different time sections can be recognized during the material evolution, short curing time and long curing time. The first has a shorter duration and is distinguished by a quick material evolution, which is characterized by a plastic behaviour similar to a consolidated clayey ground. The second one is longer and without considerable material variation. The constitutive equation for the long curing time phase describes an elastic behaviour with a material similar to concrete. This separation should not be interpreted in an absolute way because the transition from one period to the next one is not clear but, according to abovementioned features, these two different sections will be treated separately.

4.3.1. Short curing time analysis

From the author's personal experience, technical laboratory constraints and according to the raw material suppliers, the short curing time is recognized to be in the first 9 hours after the mixing phase. Accordingly, seismograms for different acquisition times were plotted, from 45 minutes to 9 hours. To deeply investigate the gelled two-component mix behaviour in the short term, which is the crucial time for job site operative reasons (the prefabricated linings required from the new ring are commonly transported 2 hours after the grout), it was decided to perform determinations every 15 minutes for 2 hours. After that, the time step for determinations was extended to 30 minutes for 4 hours and then every hour for 9 hours. The first determination was performed at 45 minutes because it was impossible to handle samples and apply the transducers before this time without irreparably damaging the still weak material.

After the test performed at 1 hour, a second test was planned and performed to ensure the right coupling between sample and transducer. Nevertheless, after just 5 minutes, the obtained seismograms showed a not negligible difference from the previous one and, for this reason, it was decided to collect this data (Traces 2 and 3, respectively, in Figure 5). Overall, 16 traces were recorded and the results are plotted in Figure 5.

[Figure 5 about here.]

The signal amplitude was tuned and amplified to highlight the behaviour of the shear-wave signal. In the first acquisition, performed 45 minutes after mixing, the shear-wave signal cannot be depicted (Trace 1); the S-wave starts to be evident after 75 minutes from the specimen preparation (Trace 4). This behaviour is consistent with the expected behaviour of the shear wave. When the sample is fresh, the shear waves cannot propagate within the specimen due to the large amount of water not yet involved in the cement hardening reaction. When the free water of the sample decreases because of the reaction progress (the weight of the sample is not changing), the first arrival of the shear-wave can be observed. As the curing time increases, the travel times tend to decrease gradually and, finally, stabilization close to 450 μs is reached at 9 hours.

Converting the travel time in seismic velocity, the shear wave velocities were computed, obtaining data ranging between 80 to 300 m/s (respectively after 45 minutes and 9 hours). Consequently, values of dynamic shear modulus were computed using Equation 2 and the outcomes are shown in Figure 6. The dynamic shear modulus (G) ranged between 8 and 110 MPa.

[Figure 6 about here.]

The computed values between 2.5 and 3.5 hours of curing time are very similar (Traces 8, 9 and 10 in Figure 6). Considering the two-component nature, the shrinkage phenomenon should not be underestimated and for tests from 2.5 to 3.5 hours, the coupling between sample and transducers has not been enough to permit a right transmission-reception of signals.

Concerning the compressional wave signal, the travel time was never detected from analysing the outcomes reported in Figure 5. Consequently, other tests were performed, tuning and amplifying signals to estimate the travel time of the P-waves that were assessed as stable in time and close to 90 μs. This is consistent with the expected behaviour of the compressive wave and comes from the high sample water content that dominates the transmission P-waves phenomenon. Converting the travel time in seismic velocity, the compression wave velocities were computed, obtaining a value close to 1500 m/s.

Regarding values of the bulk modulus (K), Poisson's ratio (ν) and dynamic Young's modulus (E), Equations 1, 3 and 4 were used, respectively, and the computed values are reported in Table 2.

[Table 2 about here.]

It should be taken into account that the Vp is affected by an uncertainly of ±15 m/s due to the travel time measures that produced a marginal fluctuation of the K parameter (less than 5%). The ν parameter was not significantly affected by the so barely appreciable fluctuation; consequently, E values are also relatively stable.

4.3.2. Long curing time analysis

From the authors' personal experience, technical laboratory constraints and according to raw material suppliers, the long curing time phase was studied carrying out tests on samples cured 1, 2 and 3 months. Traces for the acquisitions are reported in Figure 7.

[Figure 7 about here.]

Analysing the outcomes, the P-wave signal arrivals are clearly visible (at about 90–100 μs) for all the seismograms, while the S-wave signal is attenuated and is clearly readable only in the data collected after 3 months of curing. The S-wave travel times are still decreasing as the curing time increases. Indeed, after 3 months, a travel time of about 300 μs can be clearly detected. The computed outcomes from Equations 1, 2, 3 and 4 for curing times of 1 and 3 months are reported in Table 3. The analysis for 2 months was not accomplished due to the unclear S-waves dataset.

[Table 3 about here.]

After one month of curing time, the material can be considered ripe. The V_p is constant and only a moderate increase of V_s is appreciable at 3 months of curing, which leads to slight variations of ν, G, K and E.

In this case, taking into account the uncertainly due to the measure, the abovementioned slight variation may be neglected and, consequently, the material geophysical properties for 1 and 3 months of curing could be considered equal.

After the described tests, another test campaign for long curing time was scheduled and performed. To be specific, specimens cured 3, 4 and 6 months were studied and the related travel times are reported in Figure 8. Taking into account that the samples were obtained by using a component A manufactured separately and after the ones used in the previous test campaign, the test relating 3 months of curing was repeated to ensure overlapping outcomes.

[Figure 8 about here.]

Analysing Figure 8, a perfect data overlap for the 3 months cured samples can be observed with the previous test campaign; indeed, P-wave and S-wave arrivals are close to 100 and 300 μs, respectively. Unfortunately, for Traces 3 and 4 related to 4 months of curing, the shear wave signal is very weak, probably due to an unsuitable coupling between sample and transducers. Analysing Traces 5 and 6 related to 6 months of curing, no significant variations can be noticed compared to Traces 1 and 2.

5. Final remarks

The two test campaigns performed at long curing time showed good outcomes reliability. For 3 months of curing, the marked overlapping in terms of first-time arrivals both for P-wave and S-wave computed on samples cast at different times and using two different component A preparations underlines the reliability of both the mixing and casting processes.

Concerning Poisson's ratio, the freshly gelled material (short curing time) shows an initial incompressible behaviour with a

value of 0.5, while during the curing process, a decreasing trend can be observed with final values slightly lower than 0.445 after 3 months (Figure 9). The determination performed after 6 months of curing highlighted no variation. For this reason, the linear regression line reported in Figure 9 was plotted without considering the result corresponding to 6 months of curing.

[Figure 9 about here.]

The reason for these high values is the uncommon material composition that is composed of a large amount of water (more than 70% by weight). The decreasing trend is due to the chemical reaction that picks the free water (at short curing time), bonding inside the chemical structure. The impossibility of losing water for dehydration (samples are cured in water) avoids further Poisson's ratio lowering.

For the dynamic shear modulus, the growing trend spotted at short curing time describes the quick hardening reaction property of the two-component grout in the first hours of life. It can be deduced from the pertaining seismograph that before the recognition of the S-wave first time arrival after 75 minutes from the mixing phase, the material has a fluid consistency, while after this curing time it, starts to behave as a solid. Regarding the dynamic Young's modulus and its dependency on G and ν, the values follow the trends of the dynamic shear modulus with a range between 20 and 1000 MPa.

All outcomes related to the dynamic moduli are reported in Figure 10. Additionally, in this case, determinations performed after 6 months of curing highlighted no variations compared to the previous ones. Consequently, the linear regression lines were plotted without considering these values.

[Figure 10 about here.]

For the bulk modulus, considering the Vp almost constant both for short term and long terms analysis, the trend is lowering due to the increase of the dynamic shear modulus.

The data quality is clearly affected by the contact pressure between the transducers and the specimen faces. At short curing time, due to the low material strength, the maximum pressure could exceed 0.45 MPa and in some determinations, it was not sufficient to guarantee a good energy transmission to the sample and gave a consequent low quality of the detected signal. This justifies a certain degree of variability among the collected data or sometimes the impossibility to recognize the first wave arrivals. Additionally, at long curing times, not all the scheduled tests provided the expected outcomes.

6. Conclusions

The research was scheduled and performed with the aim of filling the scientific gap concerning the two-component parameters, mainly at short curing time, needed for tunnelling designers and all the stakeholders involved in the tunnelling world. The scientific literature analysis highlighted the lack of information about fundamental parameters, such as the elastic moduli and Poisson's ratio, pertaining to two-component grout. In this work, a simple approach using ultrasonic measurements was used to predict the elastic properties of specimens of two-component gelled (at short curing time) and hardened (at long curing time) grout and, according to the authors' knowledge, this is the first attempt to apply systematic monitoring on this kind of mixture used for EPB backfilling technology, even if the ultrasonic method is routinely adopted in monitoring the standard concrete hardening processes.

The travel times were evaluated both for the P-waves and S-waves to estimate the mechanical properties according to a geophysics approach. The sensitivity of the S-wave propagation (and velocity) to the curing age was highlighted for speeds ranging from about 80 to more than 500 m/s while the P-wave velocity was not affected by the curing time, with values ranged between about 1500–1685 m/s. This is completely different from the observed phenomenon occurring in concrete monitoring, where the curing provides a relevant increase of the P-wave velocity.

The authors want to highlight that this research shows preliminary results concerning the geophysical approach to two-component grout and outcomes must be verified in detail by further investigations. However, the main results could be recognized as the proof of achievement concerning the reliability of the geophysical approach to estimate the elastic properties of the tested material, with particular care for monitoring the changes of the mechanical behaviour during the hardening process. Short term monitoring has shown that P-wave velocity is not sensitive to the consolidation process, while the S-wave velocity is strongly affected by the curing time; as a matter of fact, the material is quickly changing during this phase. On the contrary, long-term monitoring shows that the material is in a stable phase. Between 1 and 3 months, a slight difference can be spotted and after 3 months, the values remain constant. According to these results, after just 1 month the hardened material has achieved steady-state elastic parameters.

Funding

This research did not receive any specific grant from funding agencies in the public, commercial, or not-for-profit sectors.

References

Agrò, G., Lo Giudice, E., Sacco, M.M., 2009. Il modulo elastico statico e dinamico del calcestruzzo, in: Conferenza AIPnD – Associazione Italiana Prove non Distruttive Monitoraggio Diagnostica.

Antunes, P., 2012. Testing procedures for two-component annulus grouts, in: Proceedings - North American Tunneling, NAT 2012, pp. 14–22.

ASTM, 2016. Standard test method for pulse velocity through concrete. Technical Report C597-16. ASTM International.

Aydin, A., 2014. Upgraded ISRM suggested method for determining sound velocity by ultrasonic pulse transmission technique. Rock Mechanics and Rock Engineering 47, 255–259. doi:10.1007/s00603-013-0454-z.

Basu, A., Aydin, A., 2006. Evaluation of ultrasonic testing in rock material characterization. Geotechnical Testing Journal 29, 117–125.

CEN, 2004. Testing concrete. Determination of ultrasonic pulse velocity. Technical Report BS EN 12504-4:2004. European Committee for Standardization.

CEN, 2016. Metodi di prova dei cementi - parte 1: determinazione delle resistenze meccaniche. CEN UNI EN 196-1:2016. European Committee for Standardization. Ente nazionale italiano di unificazione.

Càmara, J.R., 2018. Use of two-component mortar in the precast lining backfilling of mechanized tunnels in rock formations, in: Proceedings - ITA-AITES World Tunnel Congress 2018, Dubai (UAE), 20–26 April 2018.

Dal Negro, E., Boscaro, A., Barbero, E., Darras, J., 2017. Comparison between different methods for backfilling grouting in mechanized tunneling with TBM: technical and operational advantages of the two-component grouting system, in: Proceedings - AFTES International Congress 2017, Paris (FR), 13–16 November 2017.

EFNARC, 2005. Specification and guidelines for the use of specialist products for mechanised tunnelling (TBM) in soft ground and hard rock. EFNARC.

Green, R.E., 1991. Ultrasonic Testing (Nondestructive Testing Handbook). American Society for Nondestructive. chapter Introduction to Ultrasonic Testing. pp. 1–21.

Hashimoto, T., Brinkman, J., Konda, T., Kano, Y., Feddema, A., 2004. Simultaneous backfill grouting, pressure development in construction phase and in the long-term, in: Proceedings - ITA-AITES World Tunnel Congress 2004, Singapore (SG), 22–27 May 2004.

ISRM, 1977. Suggested methods for determining sound velocity. Technical Report. International Society for Rock Mechanics: Commission on Standardization of Laboratory and Field Test.

ITATech, 2014. ITAtech guidelines on best practices for segment backfilling. Technical Report 4 – May 2014. ITATech Activity Group Excavation.

Ivantchev, A., Del Rio, J., 2015. Two-component backfilling grouting for double shield TBMs, in: Proceedings - ITA-AITES World Tunnel Congress 2015, Dubrovnik (HR), 22–28 May 2015.

Khan, Z., Cascante, G., Hesham El Naggar, M., 2011. Measurement of dynamic properties of stiff specimens using ultrasonic waves. Canadian Geotechnical Journal 48, 1–15. doi:10.1139/T10-040.

McCann, D.M., Forde, M.C., 2001. Review of NDT methods in the assessment of concrete and masonry structures. NDT&E International 34, 71–84. doi:10.1016/S0963-8695(00)00032-3.

Novin, A., Tarighazali, S., Forughi, M., Fasihi, E., Mirmehrabi, S., 2015. Comparison between simultaneous backfilling methods with two components and single component grouts in EPB shield tunneling, in: Proceedings - ITA-AITES World Tunnel Congress 2015, Dubrovnik (HR), 22–28 May 2015.

Peila, D., Borio, L., Pelizza, S., 2011. The behaviour of a two-component backfilling grout used in a tunnel-boring machine. Acta Geotechnica Slovenica 8, 5–15.

Peila, D., Chieregato, A., Martinelli, D., Salazar, C.O., Shah, R., Boscaro, A., Negro, E.D., Picchio, A., 2015. Long term behavior of two component back-fill grout mix used in full face mechanized tunneling. Geoingegneria Ambientale e Mineraria 144, 57–63.

Pelizza, S., Peila, D., Borio, L., Dal Negro, E., Schulkins, R., Boscaro, A., 2010. Analysis of the performance of two-component back-filling grout in tunnel boring machines operating under face pressure, in: Proceedings - ITA-AITES World Tunnel Congress 2010, Vancouver (CA), 14–20 May 2010.

Pelizza, S., Peila, D., Sorge, R., Cignitti, F., 2012. Geotechnical aspects of underground construction in soft ground. Taylor&Francis. chapter Back-fill grout with two component mix in EPB tunneling to minimize surface settlements: Rome metro - Line C case history. pp. 291–299.

Pellegrini, L., Perruzza, P., 2009. Sao Paulo Metro project - control of settlements in variable soil conditions through EPB pressure and bicomponent backfill grout, in: Proceedings - Rapid Excavation and Tunneling Conference 2009, pp. 1137–1153.

Popovics, J.S., 2003. NDE techniques for concrete and masonry structure. progress in structural engineering and materials. Progress in Structural Engineering and Materials 5, 49–59.

Schulte-Schrepping, C., Breitenbücher, R., 2019. Two-component grouts with alkali-activated binders, in: Proceedings - ITA-AITES World Tunnel Congress 2019, Naples (I), 3–9 May 2019.

Shah, R., Lavasan, A.A., Peila, D., Todaro, C., Luciani, A., Schanz, T., 2018. Numerical study on backfilling the tail void using a two-component grout. Journal of Materials in Civil Engineering 30. doi:10.1061/(ASCE)MT.1943-5533.0002175.

Strurrup, V.R., Vecchio, F.J., Caratin, H., 1984. Pulse velocity as a measure of concrete compressive strength, in-situ non-destructive testing of concrete, in: Proceedings - In-Situ Non-Destructive Testing of Concrete. American Concrete Institute, Detroit (USA), pp. 201–227.

Thewes, M., Budach, C., 2009. Grouting of the annular gap in shield tunneling – an important factor for minimisation of settlements and production performance, in: Proceedings - ITA-AITES World Tunnel Congress 2009, Budapest (HU), 23–28 May 2009.

Todaro, C., Bongiorno, M., Carigi, A., Martinelli, D., 2020. Short term strength behavior of two-component backfilling in shield tunneling: comparison between standard penetrometer test results and UCS. Geoingegneria Ambientale e Mineraria 159, 33–40.

Todaro, C., Bongiorno, M., Martinelli, D., 2021. Two-component backfilling technology: a comparison study between laboratory and job site scales. Accepted for AFTES International Congress 2021, Paris (FR), 6–8 November 2021.

Todaro, C., Peila, L., Luciani, A., Carigi, A., Martinelli, D., Boscaro, A., 2019. Two component backfilling in shield tunneling: laboratory procedure and results of a test campaign, in: Proceedings - ITA-AITES World Tunnel Congress 2019, Naples (I), 3–9 May 2019, pp. 3210–3223. doi:10.1201/9780429424441-340.

Youn, B.Y., Breitenbücher, R., 2014. Influencing parameters of the grout mix on the properties of annular gap grouts in mechanized tunneling. Tunnelling and Underground Space Technology 43, 290–299. doi:10.1016/j.tust.2014.05.021.

Zarei, Y., Uromeihy, A., Reza Nikoodel, M., Fathollahy, M., 2019. A testing procedure for determining ultrasonic wave velocity. Bollettino di Geofisica Teorica ed Applicata 60, 433–442. doi:10.4430/bgta0272.

Zarrin, A., Zare, S., Jalali, S.M.E., 2015. Backfilling grouting with two-component grout - case study Tehran Metro Line 7 east-west lot, in: Proceedings - ITA-AITES World Tunnel Congress 2015, Dubrovnik (HR), 22–28 May 2015.

List of Figures

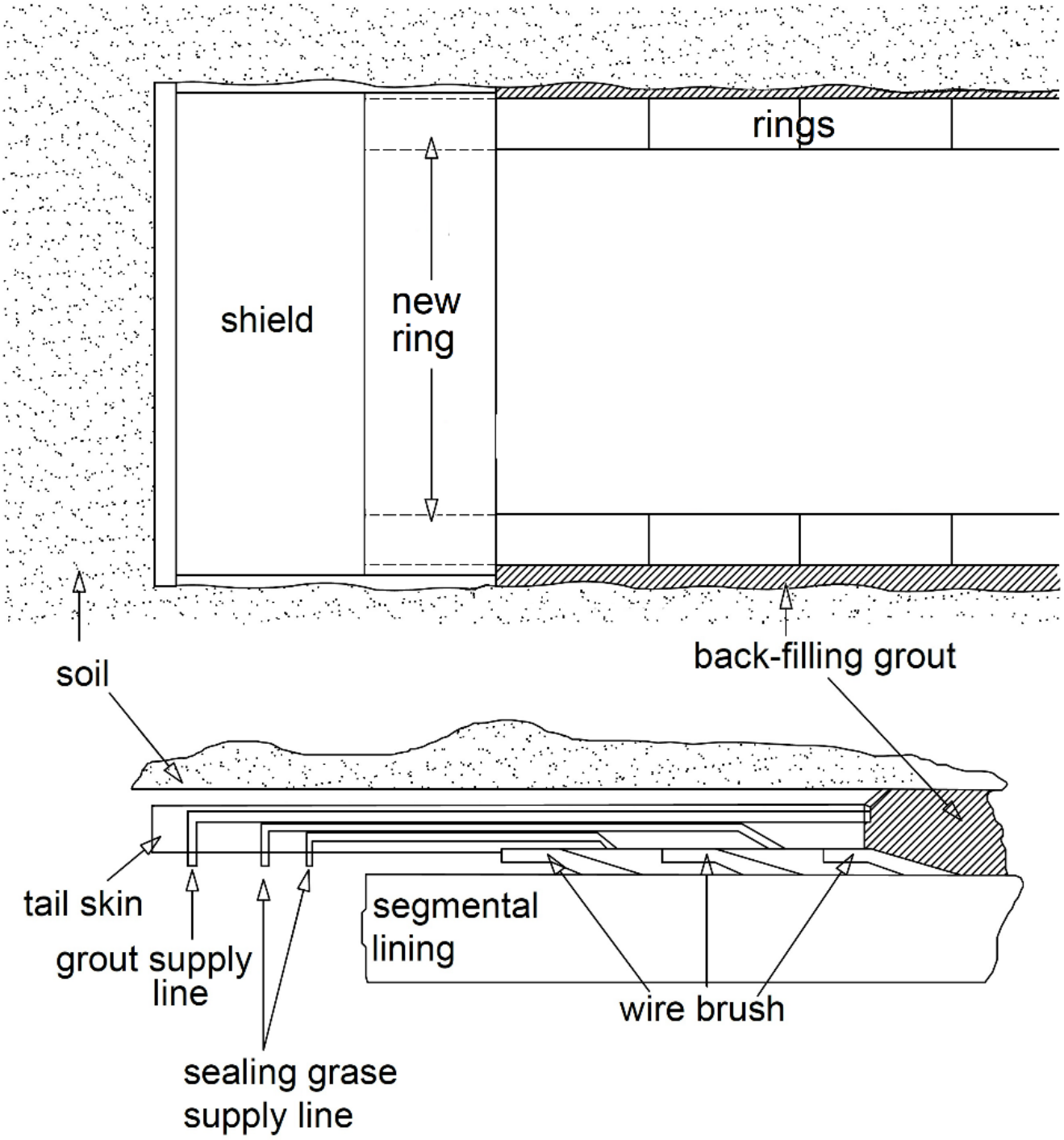

Figure 1: Simplified scheme of the backfilling system: longitudinal section of a shield machine (top) and the injection system (bottom). The backfilling grout is highlighted by the parallel line fill. The dimensions are not in real scale.

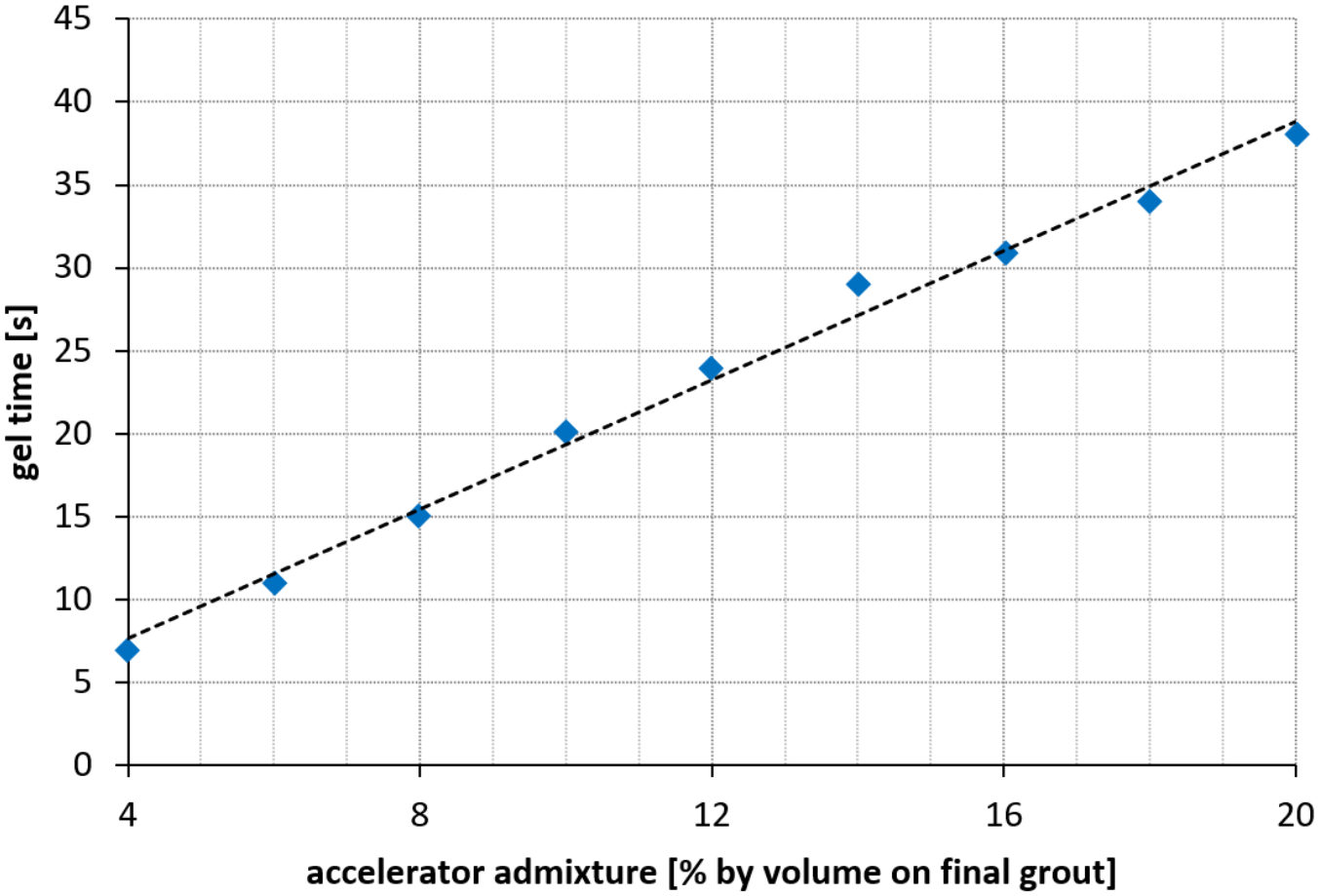

Figure 2: Example of gelling time trend as a function of the accelerator admixture percentage by volume on final grout (modified from Todaro et al. (2019)).

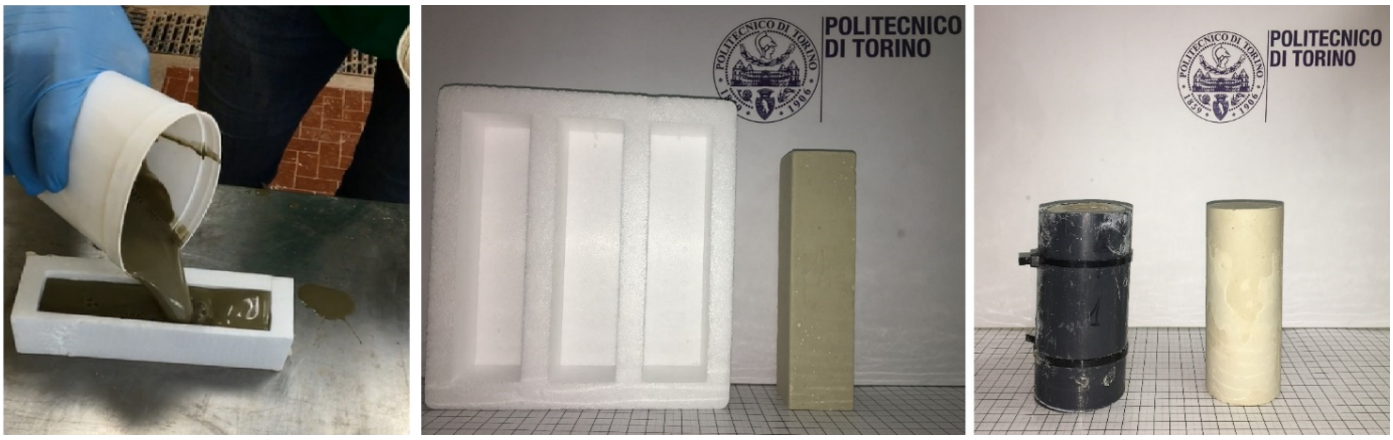

Figure 3: Casting of a prismatic sample, on the left. Example of used moulds and corresponding samples: cylindrical mould model on the right (internal diameter ϕ = 52 mm, height = 130 mm) and prismatic one (l = 40 mm, height = 160 mm) in the centre. The squares on the base background are 1 cm^2.

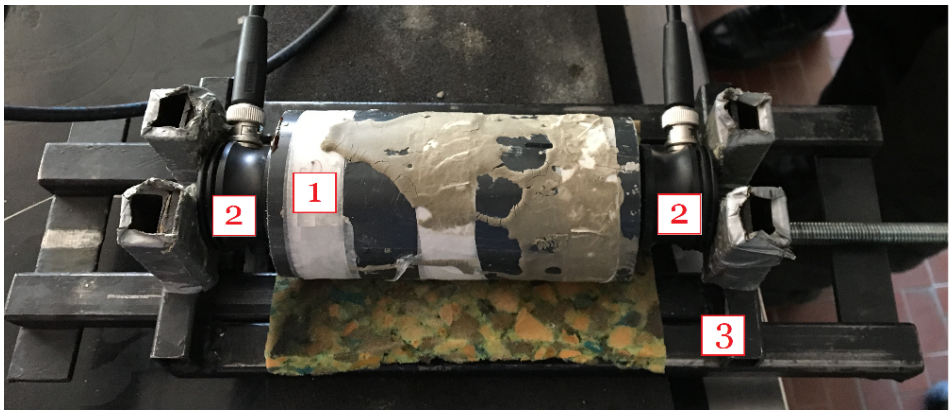

1. two component sample, covered by the PVC mold

2. transducers

3. laboratory manual press

Figure 4: Photograph of the pulse velocity test arrangement with direct transmission approach. The depicted cylindrical sample was used for the short-term analysis.

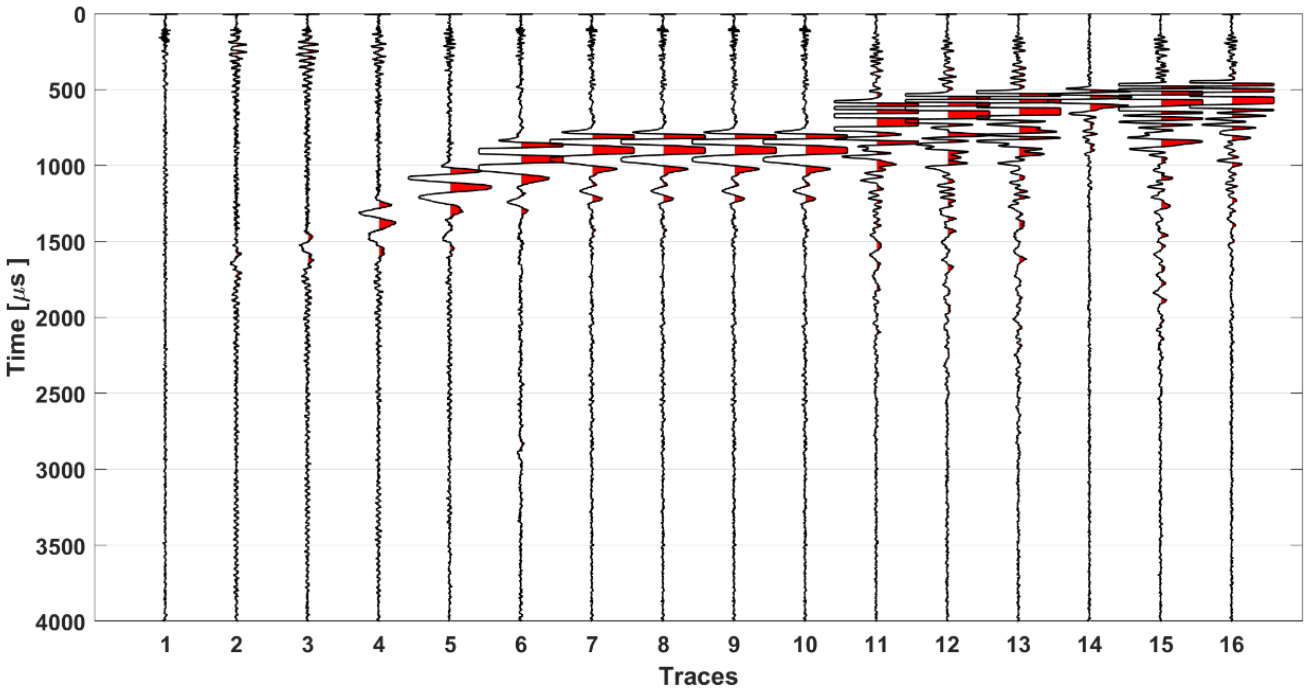

Figure 5: Seismograms for different curing times. The first trace (Trace 1) is for 45 min of curing, while the last trace (Trace 16) is for 9 hours. The most energetic signal, highlighted by the red, refers to the S-waves.

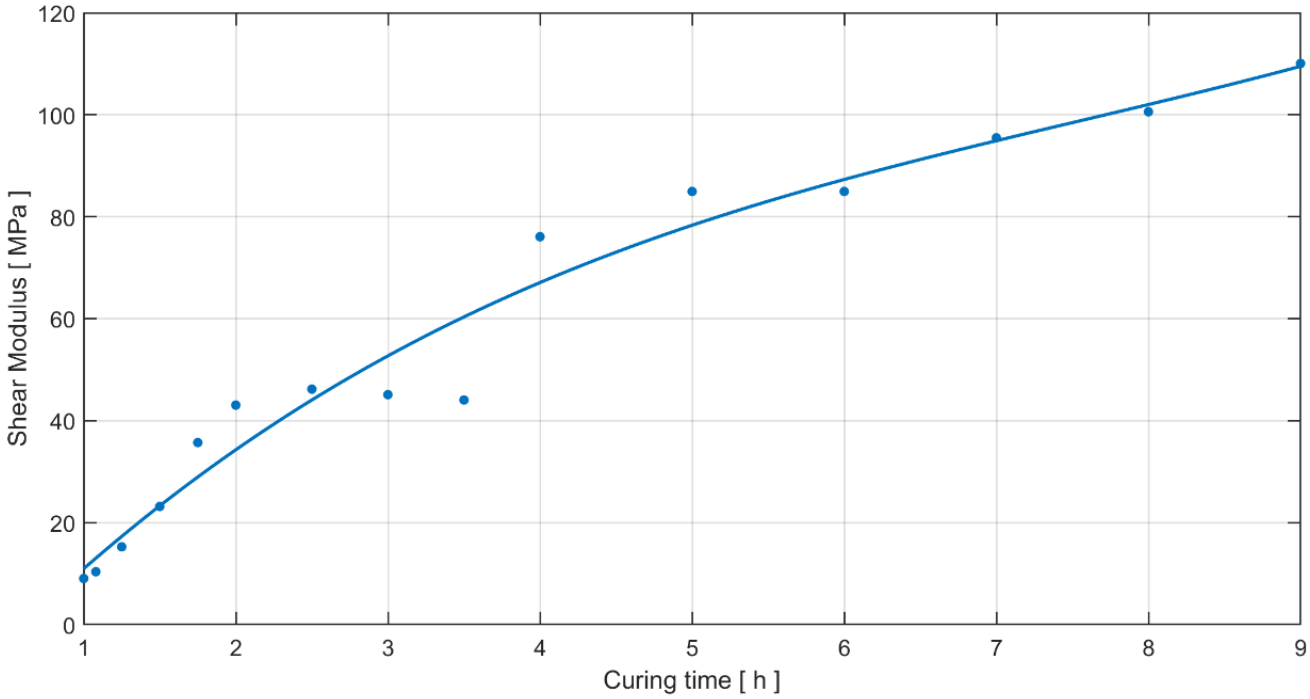

Figure 6: Dynamic shear modulus (G) versus sample curing time.

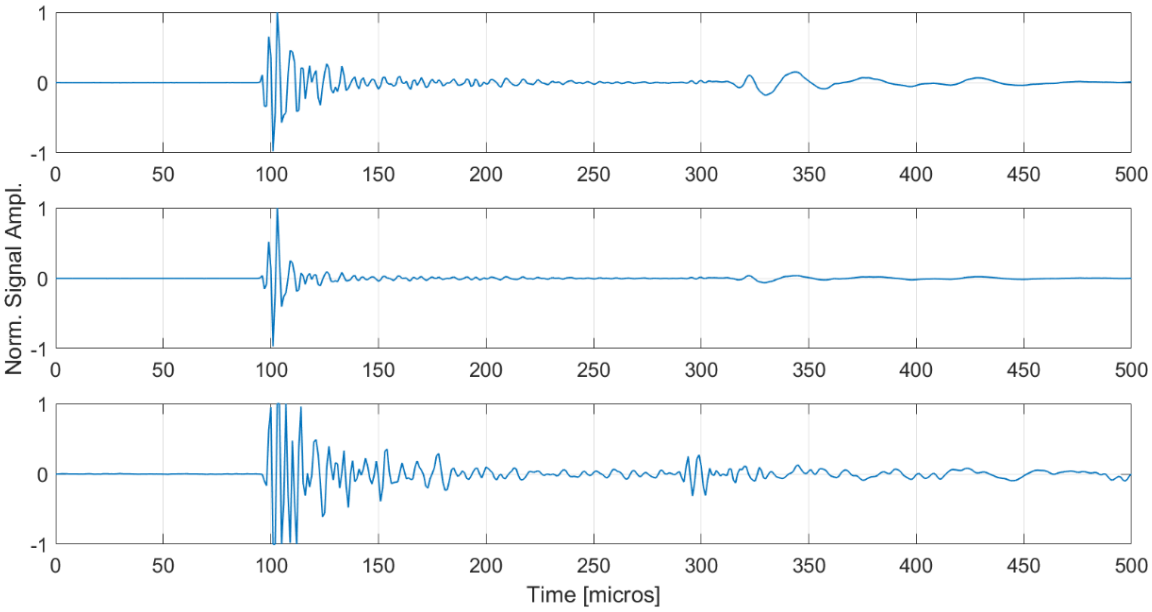

Figure 7: Seismograms for signals acquired after 1, 2 and 3 months (from top to bottom).

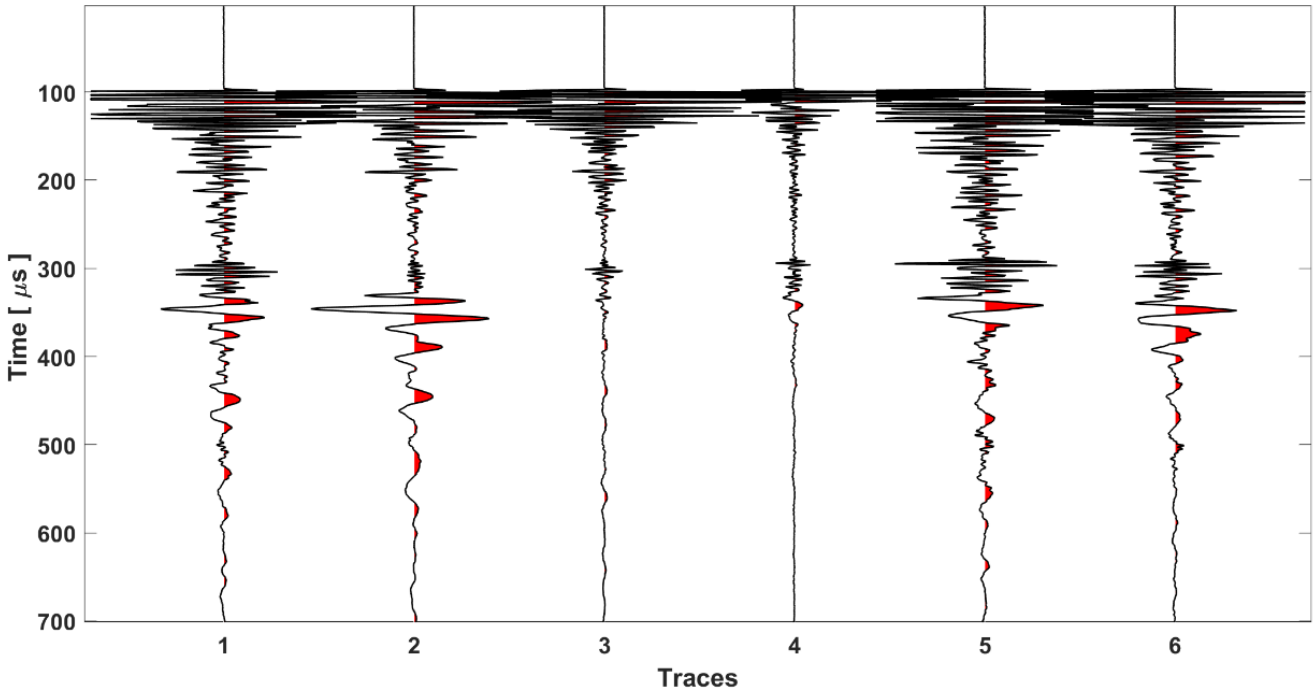

Figure 8: Seismograms of specimens cured 3 months (Traces 1 and 2), 4 months (Traces 3 and 4) and 6 months (Traces 5 and 6).

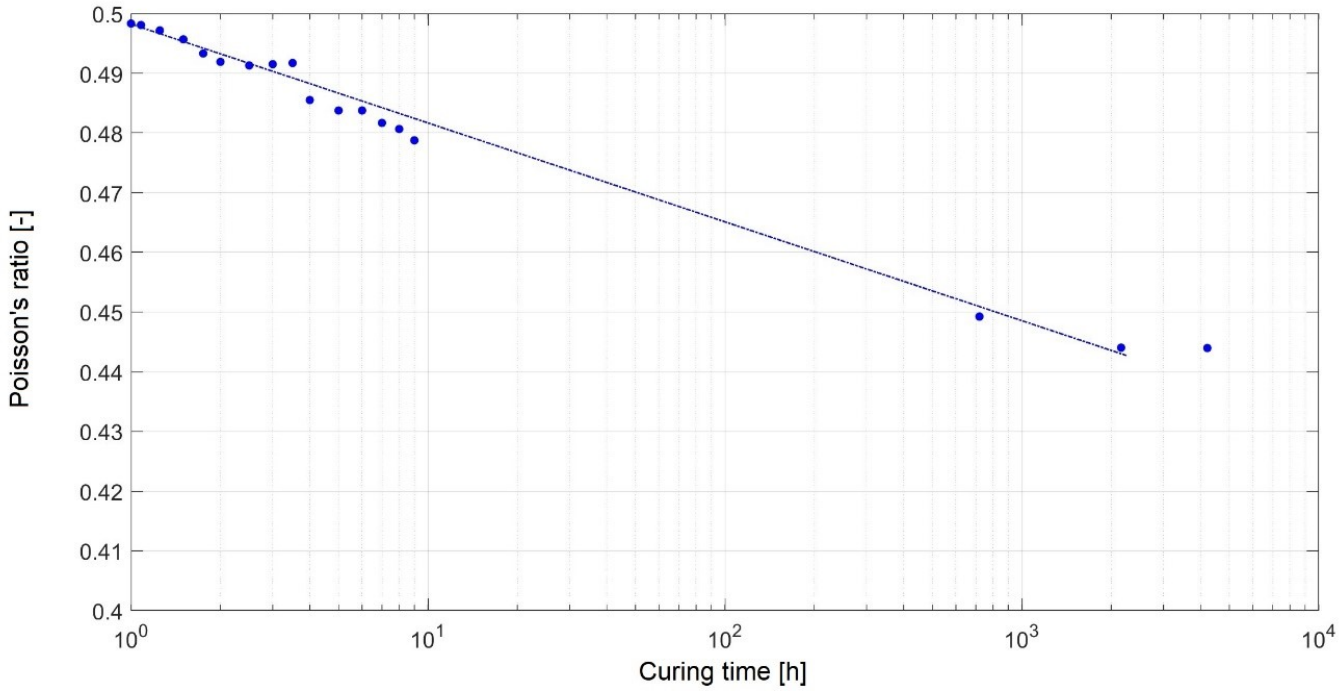

Figure 9: Poisson's ratio trend as a function of the curing time.

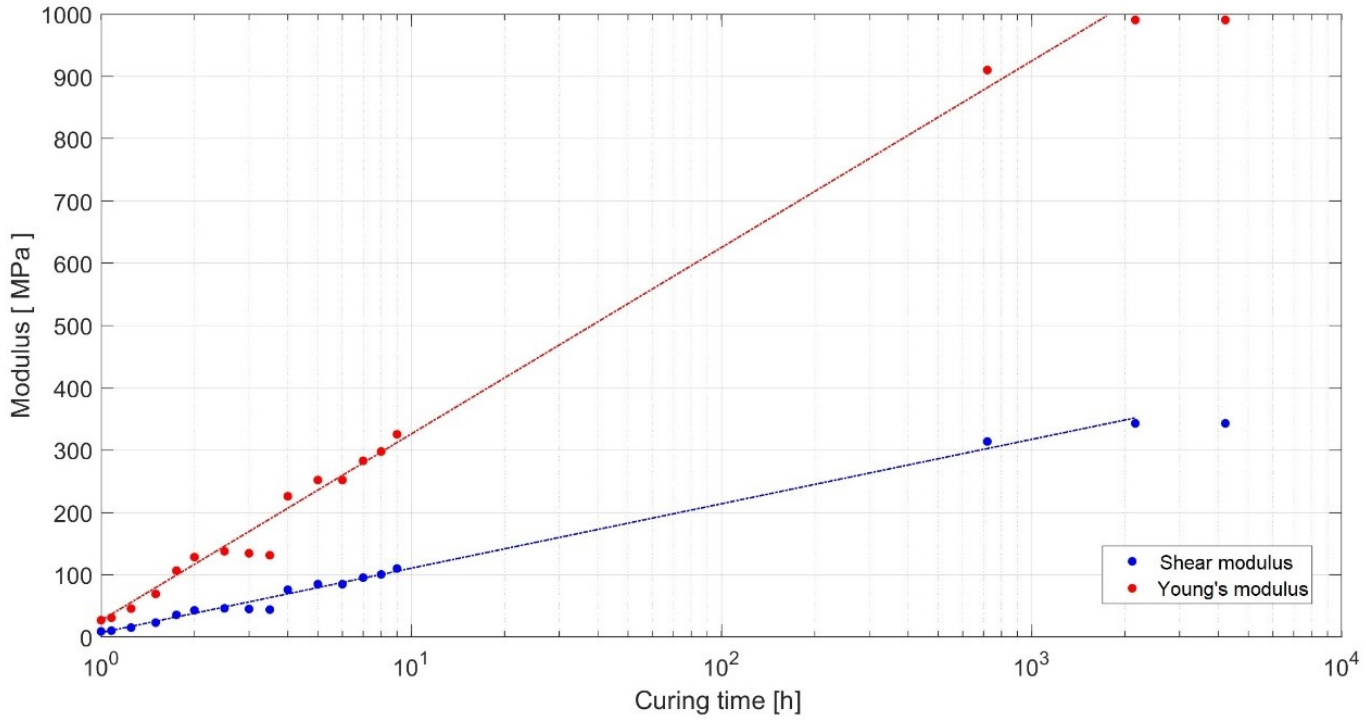

Figure 10: Dynamic Young's modulus and dynamic shear modulus trends as a function of the curing time.

List of Tables

Table 1: Mix design selected for the geophysical test campaign. Dosages are expressed in kg of ingredient per 1 m^3 of final hardened grout. The computed amount of ingredients expressed in grams are reported for each sample shape. The volume percentage of component B in the total volume is 6%

component	material	γ (kg/l)	kg/m^3	prismatic sample (g)	cylindrical sample (g)
A	cement (52.5 R, type I)	3.1	230	59	63.5
	bentonite	2.7	30	7.7	8.3
	water	1	853	217.8	234.9
	retarding/fluidifying agent	1.22	3.5	$\simeq$1	$\simeq$1
B	accelerator	1.37	81	21	22.7

Table 2: Outcomes for the short curing time in terms of pulse velocities (V_p and V_s), Poisson's ratio (ν), dynamic shear modulus (G), bulk modulus (K) and dynamic Young's modulus (E).

	45 min of curing	9 hours of curing
V_p (m/s)	1500	1500
V_s (m/s)	80	300
ν	0.5	0.48
G (MPa)	8	110
K (MPa)	2703	2570
E (MPa)	24	312

Table 3: Outcomes for 1 and 3 months of curing time in terms of pulse velocities (V_p and V_s), Poisson's ratio (ν), dynamic shear modulus (G), bulk modulus (K) and dynamic Young's modulus (E).

	1 month	3 months
V_p (m/s)	1685	1685
V_s (m/s)	510	533
ν	0.45	0.445
G (MPa)	314	343
K (MPa)	3000	2964
E (MPa)	909	990